# Search for nuclear excitation by laser-driven electron motion

J. A. Bounds and P. Dyer
*Physics Division, Los Alamos National Laboratory, Los Alamos, New Mexico 87545*
(Received 22 May 1992)

It has been proposed that a nucleus may be excited by first exciting the atom's electrons with UV photons. The incident photons couple to the electrons, which would then couple via a virtual photon to the nucleus. As a test case, experiments with $^{235}$U have been performed. A pulsed infrared laser produces an atomic vapor of $^{235}$U which is then bombarded by a high-brightness UV laser beam. The resulting ions are collected. The first excited nuclear state of $^{235}$U has a 26-min half-life and decays by internal conversion, resulting in emission of an atomic electron. These conversion electrons are detected by a channel electron multiplier. An upper limit of $4.0\times10^{-5}$ has been obtained for the probability of exciting the nucleus of a $^{235}$U atom that is in the 248-nm UV beam for 700 fs at an irradiance in the range of $1.0\times10^{15}$ to $2.5\times10^{15}$ W/cm$^2$.

PACS number(s): 23.20.Nx, 32.80.Wr

## I. INTRODUCTION

With current high-brightness lasers the electric field of the laser beam is the same order of magnitude as the electric field binding the electrons to the nucleus. Atomic physics experiments in this new regime have led to observation of a range of interesting phenomena: production of very high ionic charge states, "above-threshold ionization" where the electron in the continuum picks up the energy of additional photons, and production of radiation of very high harmonics of the driving field.

It has been proposed that the nucleus itself, in the induction-zone field of the laser-excited electrons, may be excited [1]. Such an excitation would not be a direct absorption of photons by the nucleus (because the wavelength of the photons far exceeds the size of the nucleus), but would be a Coulomb excitation by the excited electrons proceeding via virtual photons exchanged with the nucleus. The nonlinear spatial and temporal response of an atom to intense laser fields might lead to amplification of the laser field at the nucleus and to fields at the nucleus of multipolarity higher than one [2]. These considerations have been motivated largely by the desire to induce nuclear transitions of isomeric states, as required for a gamma-ray laser [3].

For investigating this laser-atomic-nuclear coupling, a search for excitation of the $^{235}$U nucleus via a high-brightness ultraviolet (UV) laser has been carried out. The signature for exciting the nuclear isomeric state is its delayed nuclear radiation. The nuclear excitation is sought in a collision-free environment to facilitate interpretation of the results; the nucleus is to be excited only by electrons of its own atom. The $^{235}$U nucleus was chosen for our first experiment, as it has an extremely low first-excited-state energy of 77 eV. The $^{235}$U ground state has spin and parity $\frac{7}{2}^-$; the first excited state, $\frac{1}{2}^+$. This excited state, having a 26-min half-life, decays by internal conversion resulting in emission of an atomic electron. These conversion electrons have a distribution of energies up to 77 eV.

This experiment was undertaken simultaneously with theoretical calculations of the same effect. Early speculations by Biedenharn *et al.* [1], assuming collective motions of the electrons, indicated transition probabilities (per laser pulse) of order 0.1 for this $^{235}$U case, for laser irradiances of order $10^{17}$ W/cm$^2$. In a first paper by Berger *et al.* [4], the electrons were treated as a classical gas acted upon by the electric field of the laser. No binding by the nucleus and no electron-electron interactions were included. An upper limit of $10^{-6}$ was obtained for the $^{235}$U nuclear transition probability in a 300-cycle long (250-fs) laser pulse of irradiance $7\times10^{16}$ W/cm$^2$ and wavelength 248 nm. In a second paper by Berger *et al.* [5], electron motion in the external sinusoidal field of the laser was treated quantum mechanically in a model where the Coulomb field of the nucleus was described by a harmonic oscillator. No electron-electron interactions were included. The electron-nucleus interaction was described perturbatively. This calculation yielded extremely low transition probabilities: only $10^{-11}$ per laser pulse of 300-cycle duration even at $10^{21}$ W/cm$^2$ for the $^{235}$U multipolarity-3 case. Hartmann *et al.* [6] have also modeled the laser-electronic-nuclear interaction, but have not calculated transition rates for the $^{235}$U$^m$ case. The present experiment measures nuclear excitation probabilities at lower laser irradiances, but with a sensitivity much higher than that required by the Biedenharn 0.1 value, though lower than that required by the values of Berger *et al.*

The laser coupling of the present search is fundamentally different from that of the experiment of Izawa and Yamanaka [7]. In their investigation, a $^{235}$U plasma was produced by high-power infrared laser bombardment of solid material, and excitation of the 77-eV isomer was sought. Izawa and Yamanaka claimed to see this excitation, and the result was interpreted as either inverse internal electron conversion (IIEC) [8] or as nuclear excitation by electron transition (NEET) [7]. However, this experiment was repeated by Arutyunyan *et al.* [9], with a null result. In the current experiment, a uranium vapor

 

was irradiated. The electron density so important to IIEC or NEET was greatly reduced compared to the above two experiments, so that neither of these two effects were measurable.

## II. EXPERIMENTAL METHOD

One of the difficulties in performing this experiment lies in the short range of the very low-energy internal conversion electrons and the long half-life involved. After irradiation by the UV laser, the uranium atoms must be collected on a surface. If the deposit is too thick, most of the conversion electrons will not exit the surface. Because it is difficult to make an atomic vapor pulse of less than a microsecond in duration, whereas the ultraviolet laser pulse is only 1 ps long, it is necessary to select only those atoms that have interacted with the UV beam in order to achieve high sensitivity. In this experiment, the ions made by the UV beam are swept out of the atomic vapor with an electric field (leaving any neutral atoms behind, including atoms that have not interacted with the UV beam). Little loss of yield results, as essentially all of the atoms that see the intense region of the UV laser beam lose at least one electron.

The scheme of the experiment is thus to bombard a vapor of $^{235}$ U atoms for about 30 min with a few-Hz high-field UV laser, collect ions formed, turn off the lasers, and detect delayed electrons from the nuclear decay. Systematics of beam parameters and gas densities were determined by time-of-flight measurements of the various charge states of uranium and argon. Decay measurements were made with vapors of $^{235}$U and $^{238}$U (as a control). A schematic diagram of the vacuum chamber (primarily stainless steel sealed by copper gaskets pumped by turbomolecular and titanium sublimation pumps) is shown in Fig. 1.

After initial trial runs at the University of Illinois at Chicago, the experiment was moved to Los Alamos. The 248-nm (5 eV photon energy) high-brightness UV beam was produced by the Los Alamos Bright Source I KrF laser system [10]. The pulse energies at the uranium target were typically 10 mJ, with a range extending from 5 to 15 mJ. Pulses were 700 fs long, as determined by two-photon ionization in nitric oxide gas, and the repetition rate was 5 pulses per second. The beam was apertured down to 29 mm, passed through the vacuum chamber, and focused back into the interaction region by a 5-cm diameter paraboloid mirror of focal length 5 cm. This mirror was mounted outside the vacuum chamber to protect it from uranium vapor deposits. The two vacuum chamber windows were made of calcium fluoride [11] to reduce two-photon absorption and were antireflection coated.

The $^{235}$U vapor was formed by laser vaporization. A 3-mm-diameter, 5-mm-long uranium slug was supported in a small tantalum collet in vacuum, about 1.2 cm from the UV beam focal region. Data were acquired with two slugs, one composed of 93% enriched $^{235}$U, and one of $^{238}$U (depleted in $^{235}$U). A $CO_2$ laser with a pulse energy of about 150 mJ and a pulse width of 35 $\mu$s was focused by a lens of focal length 25 cm onto the end of the slug and was synchronized to trigger just before the UV laser. The timing between the two laser beams was optimized by maximizing the number of collected ions. Background gas pressure was typically $2\times10^{-8}$ torr.

Two 5-cm by 5-cm electrostatic plates, spaced 3.3 cm apart, were centered on the interaction region. Two sets of ion extraction voltages were used: the first had one plate biased at +5 kV, the other at +1 kV; the second had biases of +2.5 and −1.5 kV. The higher-voltage plate had an aperture of 5 mm diameter. Next to this aperture was a plate biased at the same potential, that

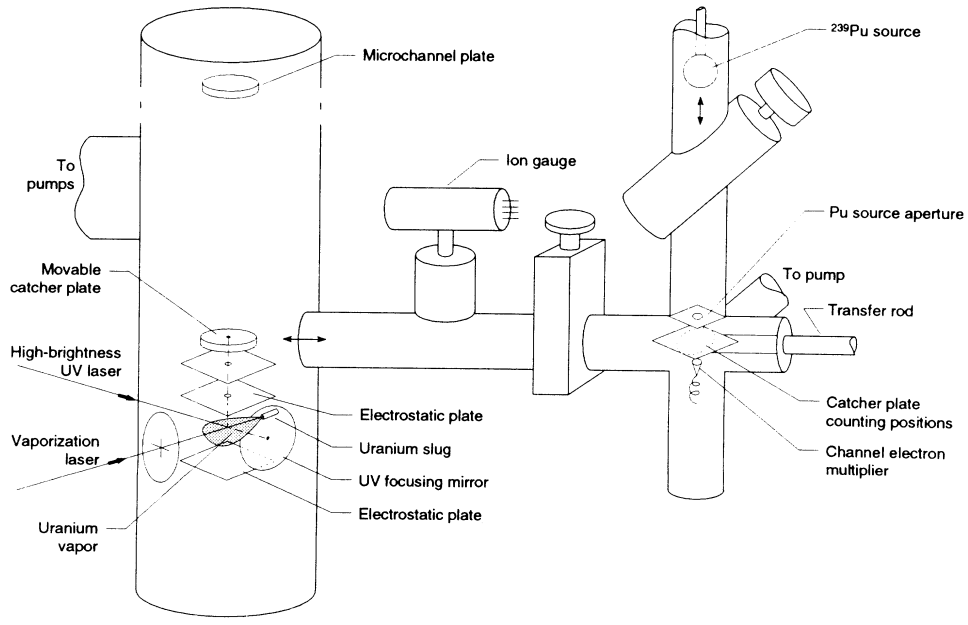


FIG. 1. Schematic diagram of the experiment.

could be moved from outside the vacuum to put any of several aperture sizes in the ion path (apertures ranging from 0.1 to 5 mm in diameter). The uranium slug and collet were biased at a potential halfway between the two electrostatic plates. For the uranium bombardment runs, ions were collected through a 1-mm-diameter aperture onto a stainless-steel catcher plate of 2.5 cm diameter (at ground potential), located 1.6 cm from the higher-voltage plate. The catcher plate was connected to a charge-sensitive preamplifier and amplifier for charge integration. This signal was digitized by CAMAC electronics and recorded with a personal computer. Calibration of the charge collection system was achieved by measuring the output voltage when the preamplifier was connected to a silicon detector looking at alpha particles of known energy from a radioactive source (in vacuum).

The time of flight of the ions was crudely measured with the catcher plate electronics. It was possible to separate three to four charge states of uranium, and to obtain the absolute numbers of ions with this system. In addition, to get a better measurement of relative yields of the high charge states (those of most interest), a microchannel plate (MCP) was mounted 60 cm above the interaction region for better time-of-flight separation. When the catcher plate was removed, the time of flight of the ions could be determined with high resolution. The MCP signal was also digitized. Examples of MCP time-of-flight spectra for argon and uranium, both taken with a 1-mm-diameter aperture, are shown in Figs. 2 and 3. All MCP measurements were made with the 1-kV, 5-kV plate voltages. In making these time-of-flight measurements, it was necessary to guard against two factors associated with the large numbers of ions formed: saturation of the MCP and space charge effects. Uncertainties from these sources were controlled by making measurements at a range of gas densities and by computer modeling of space charge effects. No attempt was made to measure absolute ion yields with the MCP. Rather, these data were used to measure the relative numbers of ions of different charge states, and absolute yields of low-charge-state ions were obtained from the catcher plate charge integration. Systematics of charge states of argon (bled in while pumping) were also studied. For both argon and uranium, time-of-flight spectra were acquired with the MCP and with the catcher plate, as a function of the position of the paraboloid mirror along the beam axis. These spectra aided in checking the focal volume dimensions. As the pressure of argon throughout the chamber could be measured with an ion gauge, comparison of argon $1^+$ and uranium $3^+$ yields (the ionization potentials being about the same for these two cases) gave an estimate of uranium density; this was required for controlling MCP saturation and space charge effects between the electrostatic plates. Typical uranium pressures were $3\times10^{-7}$ to $6\times10^{-7}$ torr. No attempt was made to measure the spatially and temporally varying uranium density directly.

During the laser bombardment period, the channel electron multiplier (CEM) for later detecting delayed electrons was physically isolated from the main chamber. This prevented its being activated by scattered light or by energetic stray particles produced by the laser beams (a problem in an earlier setup in which the CEM was in the same chamber as the bombardment, resulting in high count rates from excitations decaying with long half-lives; see the discussion of exoelectrons below). Following laser bombardment, the UV and $CO_2$ laser beams were turned off, and a vacuum-interlocked transfer rod moved the collected uranium atoms from the target chamber to the CEM chamber. The catcher was positioned 7 mm from the front of the 8-mm-diameter cone of the CEM. This front cone was biased at 300 V, so that low-energy electrons were accelerated to an energy where the quantum efficiency of the CEM was maximum. The bias across the CEM was 2500 V. An electrostatic grid was mounted in front of the CEM (about 3 mm from the cone front) to pull the electrons into the CEM. It was biased at 100 V. To map out the electron decay curve, the CEM counts were multiscaled using a CAMAC scaler, beginning about 2 min after the end of the bom-

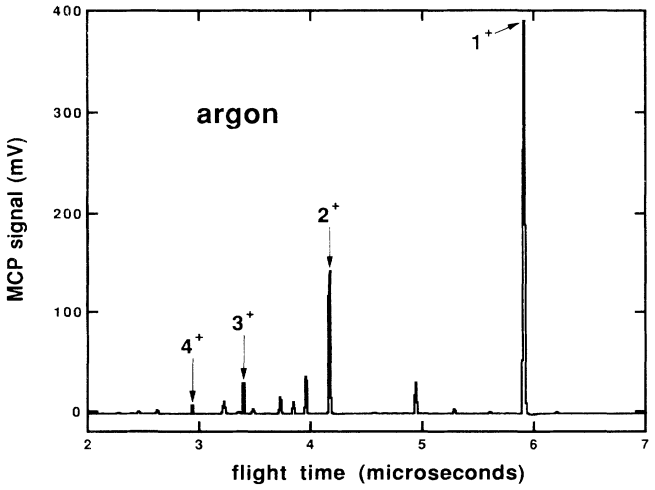


FIG. 2. MCP time-of-flight spectrum for argon, averaged over 400 laser shots.

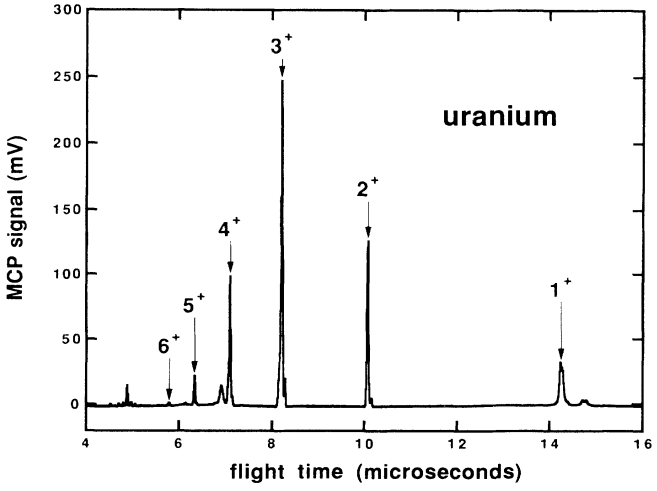


FIG. 3. MCP time-of-flight spectrum for uranium, averaged over 400 laser shots.

bardment period (the transfer time).

Before and after the set of laser-based measurements, the efficiency of the CEM was measured by depositing $^{235}U^{m}$ isomers emitted from a $^{239}Pu$ source onto the catcher plate. The source, masked to a 6-mm diameter, was placed 4 mm from the catcher plate. When the nucleus $^{239}Pu$ decays by alpha emission, the $^{235}U^{m}$ state is populated 73% of the time. The uranium nucleus recoils with an energy of 90 keV. These recoiling isomers were collected for 60 min, both under vacuum (before and after the laser measurements) and in 130 torr of argon (after the laser measurements), in the latter case with 200 V applied to the source. In the vacuum case the recoils were implanted into the catcher plate; in the argon-collection case the recoils were slowed down before being collected. Following collection, and pumpout in the argon case, the catcher plate was placed in front of the CEM, and conversion electrons were counted in the same configuration as was used in the laser experiment. The conversion electron rates before and after the laser measurements agreed to within 10%. The strength of the $^{239}Pu$ source was checked by measuring the alpha-particle emission rate (in vacuum) with a silicon surface barrier detector. The $^{239}Pu$ source was also used to set the electronic discriminator threshold and the grid voltage to maximize the signal-to-noise ratio.

Eight laser bombardments were carried out for the $^{235}U$ target (two at the 5-, 1-kV plate settings and six at the 2.5-, $-1.5$-kV settings) and seven for the $^{238}U$ target (five at 5, 1 kV and two at 2.5, $-1.5$ kV). Durations of the runs ranged from 30 to 65 min, corresponding to about 10 ns of laser bombardment. It was often necessary to adjust the $CO_2$ power to keep the uranium density constant. Delayed counting extended for about 1000 min following the bombardment. Before beginning each bombardment, several spectra were acquired: MCP time-of-flight spectra for argon and uranium, a U catcher spectrum with the $CO_2$ laser turned off, and (in the case of the $+2.5$-, $-1.5$-kV plate settings) a U catcher spectrum with the focusing mirror removed. Several U catcher spectra were acquired during the collection of ions.

## III. RESULTS

In analyzing the data, the number of collected uranium ions for the various charge states is determined, and the number of conversion electrons (or their upper limit) is extracted. The ratio of these two numbers, taking into account the efficiency for observing the $^{235}U^{m}$ decay, gives the probability that the nucleus is excited. To relate this probability to a laser beam irradiance, it is necessary to correlate charge states and irradiances.

The ratios of charge states produced were determined from the areas of the peaks in the MCP time-of-flight spectra. These areas were corrected for MCP gain according to the argon data of Hellsing *et al.* [12], taking differences in gain as depending on the varying kinetic energy (3 keV times charge) with which ions of different charge states hit the MCP. The gains for the various uranium charge states, divided by that for charge state 3, were thus taken to be 0.75 ($2^{+}$), 1.20 ($4^{+}$), and 1.36 ($5^{+}$).

The absolute yields for the lower charge states were extracted from the catcher spectra (having poor time resolution) by a nonlinear least-squares fit to the spectra. Before fitting, a $CO_2$-laser-off spectrum (no uranium vapor) was subtracted from the spectrum acquired during bombardment. This eliminated noise from the UV laser firing. For the fits, a line shape was derived from a catcher spectrum taken with the mirror moved axially off center, where mostly $1^{+}$ charge states were collected. The spectra were fitted with the sum of five lines (charge states $1^{+}$ through $5^{+}$), where the variables were the five amplitudes, the width of the line shape after convoluting it with a Gaussian shape, the slope and intercept of the flight-time calibration, a constant background, and (in the case of the $+2.5$-, $-1.5$-kV plate settings) a normalization factor for the amount of focusing-mirror-out background subtracted (from ions made by the unfocused beam on the way to the mirror). In the case of the 5-, 1-kV plate settings, the region between the $1^{+}$ and $2^{+}$ peaks, where most of the mirror-out background occurs, was omitted from the fit. An example of a fit for a $+2.5$-, $-1.5$-kV spectrum is shown in Fig. 4. No attempt was made to use $1^{+}$ data, as there was a mirror-out contribution, and as the $1^{+}$ yields were so high that saturation effects could be present in the MCP data. In analyzing the catcher data, the areas for $2^{+}$ through $5^{+}$ were added, taking into account the charge states in converting from electrical signal to number of particles. Combining these results with the MCP ratios gave absolute yields for the charge states $2^{+}$ through $5^{+}$. The total number of ions collected during the six $+2.5$-, $-1.5$-kV runs were $8\times10^{9}$ ($2^{+}$), $1\times10^{10}$ ($3^{+}$), $3\times10^{9}$ ($4^{+}$), and $5\times10^{8}$ ($5^{+}$).

In Fig. 5 are shown the electron counts in the CEM as a function of time following start of counting for $^{235}U$ isomers produced by decay of $^{239}Pu$, for the sum of the $^{235}U$ laser bombardments, and for the sum of the laser bom-

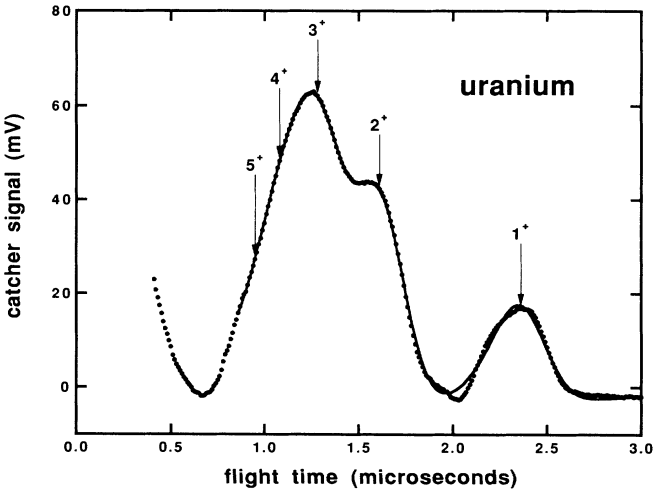


FIG. 4. Time-of-flight spectrum for uranium charge integrated at the catcher plate, averaged over 400 laser shots. The data (points) have already had $CO_2$-laser-off and focusing-mirror-out backgrounds subtracted. The solid line shows a fit to the data, as described in the text, used to extract the area under the $2^{+}$ through $5^{+}$ charge-state peaks.

bardments of the control target $^{238}U$. The signature for $^{235}U$ excitation is the existence of a 26-min half-life component in the $^{235}U$ decay curve, but not in the $^{238}U$ decay curve. For both uranium isotopes it is observed that the count rate shows a rapid falloff with a decay time of a few minutes, and some variation at later times.

Much of this structure is attributed to exoelectron emission [13]. This is emission of electrons from a solid that is relaxing after having been perturbed, for example, by mechanical deformation, by irradiation by electromagnetic radiation, or (as is presumably the case here) by ion bombardment. This delayed-electron phenomenon has been known for several decades, but the detailed emission mechanisms for this complex phenomenon are poorly understood. It is not known whether the electrons come from the surface or from the bulk of the solid, as few ultrahigh vacuum experiments have been carried out to isolate surface phenomena.

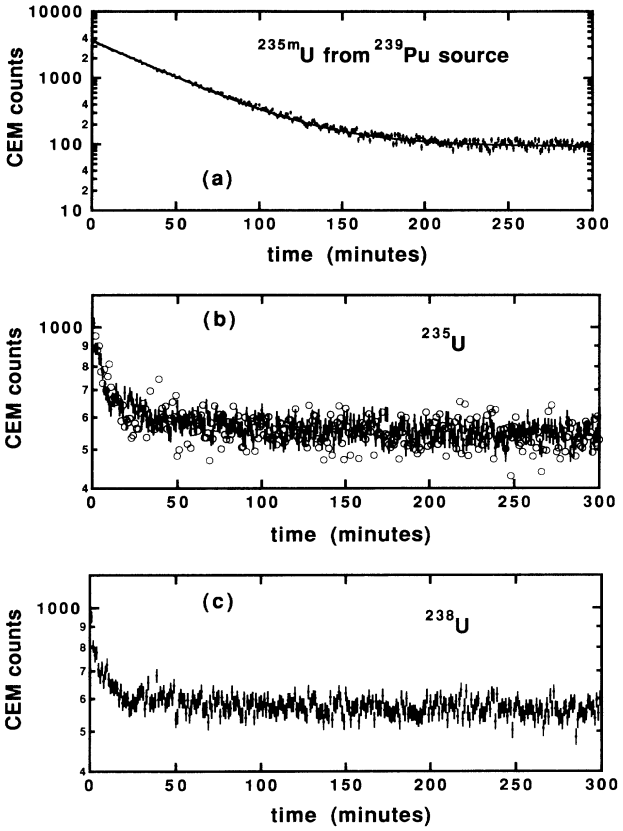


FIG. 5. Decay spectra: (a) conversion-electron decay curve for $^{235}U^{m}$ isomers stopped on the catcher plate after recoiling into argon gas from a $^{239}$Pu source, the solid line being a fit to the data, where the amplitude of a constant background and the amplitude of an exponential (with half-life constrained to 26 min) were varied; (b) electron decay curve following $^{235}U$ bombardment (solid points with error bars) summed over all runs; (c) electron decay curve following $^{238}U$ bombardment summed over all runs. In (b), the open circles show a fit with the sum of a constant background, an exponential of 26-min half-life, and a normalized short-decay-time component obtained from the $^{238}U$ data. The scatter of these fitted points comes from the statistical scatter of the $^{238}U$ data, as the short-decay-time component was extracted numerically from those data. (In the actual analysis, the data were divided into individual runs.)

The number of electrons depends on the solid and its past history as well as on the perturbation by, for example, incident charged particles. Here it is assumed that there is no difference in the exoelectron emission rate between $^{235}U$ and $^{238}U$ runs. Our experience here shows that in this type of experiment, and in other $^{235}U$ experiments such as that of Izawa and Yamanaka [7], it is important to perform the experiment for another isotope, in order to eliminate non-nuclear effects.

To extract the number of conversion-electron counts in the decay curves, constant backgrounds were subtracted and an "exoelectron" shape was derived from the $^{238}U$ data by summing the spectra (one shape for the 2.5-, $-1.5$-kV data and one for the 5-, 1-kV data). Each $^{235}U$ run (900 min of delayed counting) was then fitted with the sum of an exponential of 26-min half-life and the "exoelectron" shape, where the amplitudes of the two components were varied. Each $^{235}U$ run was fit separately, as different amounts of charge were collected in different runs and there were different corrections for decay during bombardments and before the beginning of counting. In the case of the $+2.5$-, $-1.5$-kV data, the individual values are scattered more than expected from purely statistical errors, presumably because the exoelectron contribution is somewhat unpredictable. The errors have been increased (by about a factor of 5.5) to make the $\chi^2$ per degree of freedom unity. In the case of the 1-, 5-kV data, where there were not enough runs to establish a distribution, the errors were multiplied by this same factor. For illustration purposes, all data have been summed in Fig. 5.

The CEM efficiency was determined from the $^{239}$Pu measurement and from a Monte Carlo calculation of electron losses in exiting the catcher plate material. This Monte Carlo calculation is described in the Appendix. The efficiency for detecting an emitted conversion electron is that measured when collecting recoils from the $^{239}$ Pu source in vacuum (0.0050) multiplied by the exit ratios given in Table I.

For each run, the number of excited $^{235}U$ nuclei were obtained from the fit results and the CEM efficiency, after correcting for decay losses during the bombardment and between the end of bombardment and the beginning of counting. The ratio to the number of collected ions gives, for each charge state, an upper limit on the probability for exciting the $^{235}U$ nucleus when the atom is bombard-

TABLE I. Electron exit ratios from a Monte Carlo calculation.

| Charge state | Plate voltages (kV) | Exit ratio |
|---|---|---|
| $2^+$ | 5,1 | 0.62 (0.24–0.96) |
| $3^+$ | 5,1 | 0.34 (0.07–0.69) |
| $4^+$ | 5,1 | 0.23 (0.03–0.58) |
| $5^+$ | 5,1 | 0.17 (0.01–0.52) |
| $2^+$ | $+2.5,-1.5$ | 3.50 (2.56–4.06) |
| $3^+$ | $+2.5,-1.5$ | 2.28 (1.77–2.37) |
| $4^+$ | $+2.5,-1.5$ | 1.55 (0.90–1.66) |
| $5^+$ | $+2.5,-1.5$ | 1.33 (0.71–1.48) |

TABLE II. Nuclear excitation probabilities for a range of UV bombardment irradiances.

| Charge State | Plate Voltages (kV) | CEM Efficiency | $P$(700 fs) | Irradiance (W/cm$^2$) |
|---|---|---|---|---|
| $2^+$ | 5,1 | $(3.1\pm1.8)\times10^{-3}$ | $(-1.1\pm1.5)\times10^{-5}$ | $(1.8\text{–}4.8)\times10^{13}$ |
| $3^+$ | 5,1 | $(1.7\pm1.5)\times10^{-3}$ | $(-1.3\pm2.0)\times10^{-5}$ | $(4.8\text{–}23)\times10^{13}$ |
| $2^+$ | +2.5,−1.5 | $(1.8\pm0.4)\times10^{-2}$ | $(4.5\pm5.5)\times10^{-7}$ | $(1.8\text{–}4.8)\times10^{13}$ |
| $3^+$ | +2.5,−1.5 | $(1.1\pm0.1)\times10^{-2}$ | $(2.9\pm4.6)\times10^{-7}$ | $(4.8\text{–}23)\times10^{13}$ |
| $4^+$ | +2.5,−1.5 | $(7.8\pm1.9)\times10^{-3}$ | $(2.1\pm2.9)\times10^{-6}$ | $(2.3\text{–}10)\times10^{14}$ |
| $5^+$ | +2.5,−1.5 | $(6.7\pm1.9)\times10^{-3}$ | $(1.8\pm2.2)\times10^{-5}$ | $(1.0\text{–}2.5)\times10^{15}$ |

ed by a 700-fs-long high-intensity 248-nm laser beam.

Ions are collected from the region of the UV beam focal waist positioned under the 1-mm aperture in the lower-voltage electrostatic plate. They have been exposed to a continuum of beam irradiances, determined by the spatial profile of the laser beam. In a sequential ionization picture, high charge states are produced in the center of the laser beam waist and lower charge states in the periphery. As it is required to know the laser beam irradiance to which the atoms of each charge state were exposed, it is necessary to know the relationship between the ionization energy and the beam irradiance required for ionization, as given by a curve based either on calculations or on measurements of multiphoton ionization systematics. This curve was taken from the one-dimensional Coulombic-barrier model of Augst *et al.* [14], in which ionization occurs when the amount of suppression of the Coulomb potential by the potential of the laser field is equal to the ionization potential of the atom or ion. In this tunneling regime, the appearance intensity is given by

$$I_{\text{app}}=cE_{\text{ion}}^4/128\pi e^6Z^2 ,$$

where $E_{\text{ion}}$ is the ionization potential, $Z$ is the charge of the resulting ion, $c$ is the speed of light, and $e$ is the charge of the electron. This equation describes well the multiphoton ionization of rare gas ions with 1-$\mu$m wavelength, 1-ps-long laser pulses [14]. It is in qualitative agreement with the 248-nm ionization data for the heavy rare gases of Gibson *et al.* [15], even though those data would not be expected to be described in the tunneling regime. The regime of the present experiment is the same as that of Gibson *et al.* In the present experiment, the $5^+$ uranium ions are expected to be close to the tunneling regime, but the lower charge states are further from it.

This tunneling formula is also supported by the numbers of argon ions of charge states $1^+$ through $4^+$ measured in the present experiment by MCP time of flight, as a function of the position of the paraboloid mirror along the beam axis. The laser beam is assumed to have a Gaussian shape [16], given by

$$W_z=W_0[1+(M^2\lambda z/\pi W_0^2)^2]^{1/2} ,$$

where $W_z$ is the radius defined by $1/e^2$ irradiance at position $z$ along the beam axis, $W_0$ is the radius at $z=0$, $\lambda$ is the wavelength, and $M^2$ describes how fast the beam expands. A nonunity $M^2$ value describes multimode structure in the beam. If the pulse length and energy are known, then the volume in which ions of a given charge state are made can be calculated for a range of beam radii $W_0$ and $M^2$ values (given the irradiance versus ionization energy curve). A qualitative match to the measured argon distribution is found for $W_0=1.5$ $\mu$m and $M^2=3$, which are reasonable values [10,17]. Future experimental work may yield better estimates of the irradiance versus ionization potential curve. For the present, in accordance with the formula of Augst *et al.*, a range of irradiances of $1.8\times10^{13}$ to $4.8\times10^{13}$ W/cm$^2$ is associated with charge 2, $4.8\times10^{13}$ to $2.3\times10^{14}$ with charge 3, $2.3\times10^{14}$ to $1.0\times10^{15}$ with charge 4, and $1.0\times10^{15}$ to $2.5\times10^{15}$ with charge 5. The ionization potentials used were those of Carlson *et al.* [18].

The results are given in Table II for the two plate-voltage settings. The one-standard-deviation errors are a quadratic sum of the (fractional) errors in the number of conversion electrons observed, the efficiency (taken as the average of the upper and lower errors), and the number of charges collected (taken as 20%). As conversion-electron losses are larger (efficiency lower) for the higher kinetic energy case, the 5-, 1-kV data are less accurate, and no results are quoted for the $4^+$ and $5^+$ cases, as the lower limits on the efficiencies are very low (see Appendix). The sensitivity of the experiment decreases with increasing laser intensity, as fewer atoms are exposed to the higher intensities. It is found, for example, that a $^{235}$U atom in a focal volume where the 248-nm irradiance ranges from $1.0\times10^{15}$ to $2.5\times10^{15}$ W/cm$^2$ (values adopted for charge state 5) for 700 fs (850 cycles) has an excitation probability $P$(700 fs) of less than $4.0\times10^{-5}$.

## IV. CONCLUSIONS

Upper limits have been placed on the nuclear excitation probability at UV laser irradiances up to $2\times10^{15}$ W/cm$^2$. The present experimental limit does not disagree with the theoretical value of Berger *et al.* [5], but does not reach the limit required for a real test. Experiments at higher laser intensities and theory of higher accuracy, including collective electron motions and screening of the laser field, are required if this laser-atomic-nuclear coupling is to be observed and understood.

## ACKNOWLEDGMENTS

We are grateful to T. S. Luk, C. K. Rhodes, and the staff at the University of Illinois at Chicago, where preliminary measurements took place. For providing the UV laser beam and for helping us set up and interpret the time-of-flight measurements, we are highly indebted to several of the staff of the Los Alamos Bright Source: D. E. Casperson, S. E. Harper, L. A. Jones, G. A. Kyrala, J.

P. Roberts, G. T. Schappert, and A. J. Taylor. R. C. Haight and G. C. Baldwin of Los Alamos participated in the early phases of this work. We are grateful for theoretical input from G. A. Rinker, L. C. Biedenharn, J. C. Solem, and M. S. Weiss. This research was supported by the Division of Advanced Energy Projects of the U.S. Department of Energy.

## APPENDIX: CEM EFFICIENCY FOR CONVERSION-ELECTRON COUNTING

When $^{239}$Pu source measurements are made with collection in vacuum, the $^{235}U^{m}$ recoils are implanted into the stainless-steel catcher plate with an energy of 90 keV less that lost in exiting the $^{239}$Pu layer. Implantation depths range from zero up to 15 nm. (The $^{239}$Pu source is thick enough that only recoils from the outside 40% of the layer have a chance to exit.) When the $^{239}$Pu measurement is made with collection in argon, the $^{235}U^{m}$ recoils are gently implanted into the surface. When $^{235}$U ions are collected during the laser bombardment, the implantation depth varies depending on the kinetic energy of the ion (3 or 0.5 kV times the charge, depending on the plate voltages) and ranges from 1 to 6 nm for charge states 2 through 5. It is thus necessary to take into account losses of electrons in the solid in determining the efficiency for a given charge state and kinetic energy using the $^{239}$Pu source data. The farther from the surface the conversion electron is generated, the less likely the electron is to reach the surface with enought energy to escape after suffering inelastic scattering energy losses. It is important to note that the calculations do not need to yield correct absolute numbers, but only ratios of numbers from varying implantation depths. The $^{239}$Pu measurement provides the absolute number.

The electron losses were modeled with a three-dimensional Monte Carlo code. All heavy-ion energy losses and ranges were determined from the TRIM89 program [19]. For the case of the $^{239}$Pu source with collection in vacuum, the code began by randomly distributing the alpha decays in depth and angle. Then the energy loss of the $^{235}U^{m}$ in exiting the Pu layer (taking into account the path length dependence on angle) was calculated. From the remaining energy the range in stainless steel (approximated as iron) was determined, and thus the depth of implantation and position of emission of the conversion electron (again taking the angle into account). For the case of the $^{239}$Pu source with collection in argon the depth of implantation was taken to be 0.1 nm. For the case of the laser bombardment runs, the implantation depth was calculated from the incident ion kinetic energy.

The next step was to follow the trajectory of the conversion electron. Given an initial electron energy (distributed as described below), and an initially random direction, the electron was moved a distance corresponding to its mean free path for inelastic scattering [20] and forced to lose energy in an inelastic scattering event. A randomly selected scattering angle and an energy loss were calculated, and a new energy and new direction cosines were assigned. A secondary electron may also be produced. The original electron was then allowed to propagate another mean-free-path length, and another inelastic scattering event occurred. The sequence continued until the electron exited or lost so much energy that it could not escape the surface. To escape, the momentum projection on the normal to the surface (relative to the bottom of the Fermi gas) must be sufficient to overcome that corresponding to the sum of the Fermi and work function energies. Next the secondary electrons were traced in the same way.

In the calculation, best values were chosen for the initial conversion-electron energy range, the scattered energy distribution, the scattering angular distribution, the Fermi energy, and the work function. In addition, the code was run for a variety of other values, and the range of efficiency ratios obtained was used to assign an error to the value. Included in the error were the values obtained with no secondary electron production.

For the work function, the value 4.7 eV for iron was chosen, but a range of 2.7 to 6.7 eV was considered. For the Fermi energy, the value 7 eV was chosen, again characteristic of iron, and a range of 5 to 9 eV was included in the error analysis. The initial electron energy was distributed randomly between 57 and 77 eV (relative to the bottom of the Fermi gas), according to the conversion-electron energy measurements of Zhudov *et al.* [21]. The code was also run for a 37 to 57 eV range, and the result included in the error. To get the distribution of scattered electron energies for an inelastic scattering event, the algorithm of Tougaard [22] was used. The code was also run for energy losses evenly distributed from zero up to the incident energy, and for probabilities increasing linearly with energy loss from zero up to the incident energy, with the values included in the error range. The scattering angle of the inelastically scattered electron (relative to the incident direction) is expected to be small when the incident energy is large, and isotropic when the energy is small. This angular distribution was parametrized by a Gaussian distribution in angle, where the root-mean-square deviation of the angle (in radians) was expressed by a constant divided by the square of the incident energy (in eV). The best value of the constant was taken to be 100, as this value gave agreement between the ratio of the number of conversion electrons observed from the $^{239}$Pu measurement in argon to the number with vacuum collection (the ratio being 9). In the error analysis, values of the constant from 0 to 400 were included. The momentum of secondary electrons was calculated as the sum of the momenta of the incident electron and an electron in the Fermi gas, less the momentum of the scattered electron. The incident electron in the Fermi gas was given a random direction and a magnitude corresponding to a kinetic energy randomly distributed in the range from zero to the Fermi energy.

The results for the ratios of numbers of electrons exiting from the implantation depth of a given charge state to the number of electrons exiting when $^{235}$U recoils are collected in vacuum from a $^{239}$Pu source in our geometry are given in Table I, where the best values are followed by numbers in parentheses indicating the range for the above parameter variation.

[1] L. C. Biedenharn, G. C. Baldwin, K. Boyer, and J. C. Solem, in *Advances in Laser Science—I,* Proceedings of the First International Laser Science Conference, Dallas, TX, 1985, edited by W. C. Stwalley and M. Lapp, AIP Conf. Proc. No. 146 (AIP, New York, 1985), p. 52; G. A. Rinker, J. C. Solem, and L. C. Biedenharn, in *Advances in Laser Science—II,* Proceedings of the Second International Laser Science Conference, Seattle, WA, 1986, edited by M. Lapp, W. C. Stwalley, and G. A. Kenney-Wallace, AIP Conf. Proc. No. 160 (AIP, New York, 1987), p. 75.

[2] J. C. Solem and L. C. Biedenharn, J. Quant. Spectrosc. Radiat. Transfer **40**, 707 (1988).

[3] G. C. Baldwin, Phys. Rep. **87**, 1 (1982); G. C. Baldwin, in *Advances in Laser Science—I,* Proceedings of the First International Laser Science Conference, Dallas, TX, 1985 [1], p. 6. See also J. Quant. Spectrosc. Radiat. Transfer **40**, (6), 1988, special issue on gamma-ray lasers.

[4] J. F. Berger, D. Gogny, and M. S. Weiss, J. Quant. Spectrosc. Radiat. Transfer **40**, 717 (1988).

[5] J. F. Berger, D. M. Gogny, and M. S. Weiss, Phys. Rev. A **43**, 455 (1991).

[6] F. X. Hartmann, D. W. Noid, and Y. Y. Sharon, Phys. Rev. A **44**, 3210 (1991).

[7] Y. Izawa and C. Yamanaka, Phys. Lett. **88B**, 59 (1979).

[8] V. I. Goldanskii and V. A. Namiot, Yad. Fiz. **33**, 319 (1981) [Sov. J. Nucl. Phys. **33**, 169 (1981)].

[9] R. V. Arutyunyan, L. A. Bol'shov, V. D. Vikharev, S. A. Dorshakov, V. A. Kornilo, A. A. Krivolapov, V. P. Smirnov, and E. V. Tkalya, Yad. Fiz. **53**, 36 (1991) [Sov. J. Nucl. Phys. **53**, 23 (1991)].

[10] J. P. Roberts, A. J. Taylor, P. H. Y. Lee, and R. B. Gibson, Opt. Lett. **13**, 734 (1988).

[11] Material Optipur, Optovac, Inc., North Brookfield, MA.

[12] M. Hellsing, L. Karlsson, H. -O. Andren, and H. Norden, J. Phys. E **18**, 920 (1985).

[13] H. Glaefeke, in *Thermally Stimulated Relaxation in Solids,* edited by P. Braunlich (Springer-Verlag, Berlin, 1979), p. 225.

[14] S. Augst, D. Strickland, D. D. Meyerhofer, S. L. Chin, and J. H. Eberly, Phys. Rev. Lett. **63**, 2212 (1989).

[15] G. Gibson, T. S. Luk, and C. K. Rhodes, Phys. Rev. A **41**, 5049 (1990).

[16] M. W. Sasnett, in *The Physics and Technology of Laser Resonators,* edited by D. R. Hall and P. E. Jackson (Adam Hilger, Bristol, 1989).

[17] G. A. Kyrala and T. D. Nichols, Phys. Rev. A **44**, R1450 (1991).

[18] T. A. Carlson, C. W. Nestor, Jr., N. Wasserman, and J. D. McDowell, At. Data **2**, 63 (1970).

[19] J. F. Ziegler, J. P. Biersack, and U. Littmark, *The Stopping and Range of Ions in Solids* (Pergamon, New York, 1985).

[20] M. P. Seah and W. A. Dench, Surf. Interface Anal. **1**, 1 (1979).

[21] V. I. Zhudov, A. G. Zelenkov, V. M. Kulakov, V. I. Mostovoi, and B. V. Odinov, Pis'ma Zh. Eksp. Teor. Fiz. **30**, 549 (1979) [JETP Lett. **30**, 516 (1979)].

[22] S. Tougaard, Surf. Interface Anal. **11**, 453 (1988).

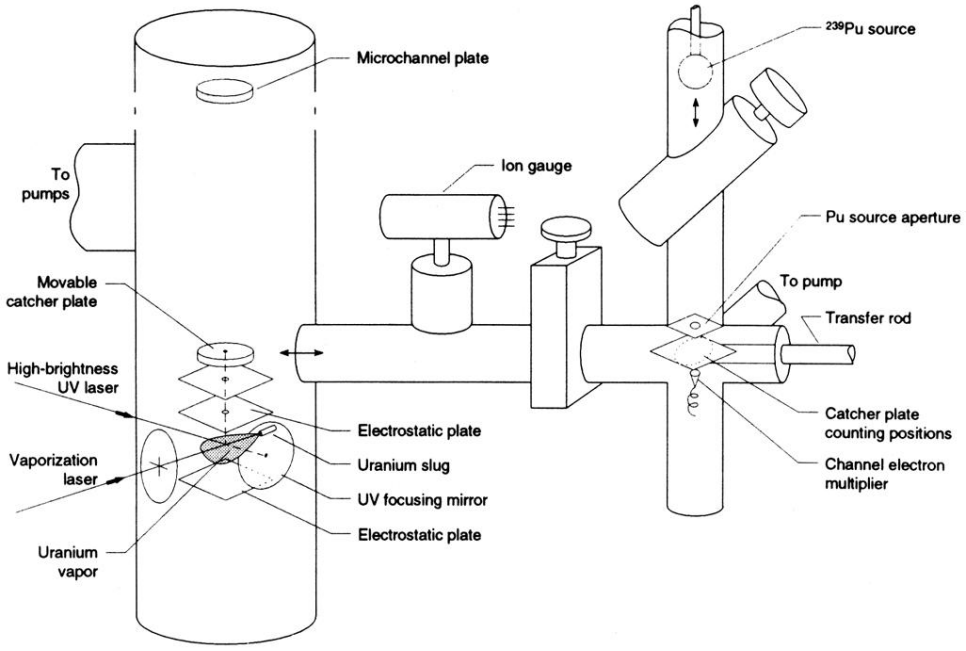


FIG. 1. Schematic diagram of the experiment.